

# DEVELOPMENT OF CU-AL-MN BASED SHAPE MEMORY ALLOYS -APPLICATION TO MEDICAL GUIDE WIRE-<sup>1</sup>

Y. Sutou<sup>2</sup>

T. Omori<sup>2</sup>

R. Kainuma<sup>3</sup>

K. Yamauchi<sup>2</sup>

K. Ishida<sup>4</sup>

## Abstract

A new type of medical guidewire with functionally graded characteristics from the tip to the end was developed using Cu-Al-Mn-based alloys. The superelasticity (SE) of the Cu-Al-Mn-based alloys can be drastically improved by controlling the grain size, and the present alloys were hardened by ageing at around 300°C. Based on these results, a Cu-Al-Mn-based core wire for a guidewire with a superelastic tip portion and a high rigid body portion was manufactured. This guidewire shows excellent pushability and torquability superior to those of stainless steel and Ti-Ni guidewires.

**Key words:** Shape memory alloy; Cu-Al-Mn alloy; Guidewire

<sup>1</sup> *Technical contribution to 62nd ABM - International Annual Congress, July 23<sup>rd</sup> to 27<sup>th</sup>, 2007, Vitória - ES – Brazil*

<sup>2</sup> *1 Tohoku University Biomedical Engineering Research Organization, TUBERO Aobayama Material Science Branch, 6-6-02 Aoba-yama, Sendai 980-8579, Japan*

<sup>3</sup> *Institute of Multidisciplinary Research for Advanced Materials, Tohoku University, 1-1 Katahira, Sendai 980-8577, Japan*

<sup>4</sup> *Department of Materials Science, Graduate School of Engineering, Tohoku University, 6-6-02 Aoba-yama, Sendai 980-8579, Japan*

## 1. Introduction

Cu-based shape memory alloys (SMAs) of the Cu-Zn- and Cu-Al-based systems are commercially attractive for the manufacture of practical applications based on the shape memory effect (SME) and superelasticity (SE) because of their low cost compared with Ti-Ni SMAs. Currently, SMAs are attracting considerable attention as core materials for medical devices such as guidewires, stents and so on [1-4]. However, conventional polycrystalline Cu-based SMAs are too brittle to be sufficiently cold-worked, which restricts the attainable SE strain to only about 2% [5,6]. The brittleness of the  $\beta$ -polycrystalline Cu-based SMAs arises from the high degree of order in the parent  $\beta$  phase, the abnormally high elastic anisotropy ratio and the coarse grains structure [5]. Therefore, many attempts have been made to improve the ductility mainly by grain refining through the addition of less-soluble alloying elements, but with limited success [5,7].

During the last decade, we have developed Cu-Al-Mn-based SMAs with a low Al content showing excellent cold-workability [8,9]. Figure 1 shows a vertical section diagram in the Cu-Al-10at.%Mn system [10]. As shown in Fig. 1, the  $\beta$  single-phase region is seen to be broadened by the addition of Mn. It can also be seen that in the  $\beta$  phase region, the two types of ordering transition temperatures indicated by  $T_c^{A2-B2}$  and  $T_c^{B2-L21}$  drastically decrease with decreasing Al content. The reason for the enhancement of ductility in Cu-Al-Mn-based SMAs is attributed to the decrease in the degree of order in the parent  $L2_1$  phase. In the composition range above 16at.% Al, the  $L2_1$  structure martensitically transforms into the 6M structure. On the other hand, in the composition range below 16at.% Al, the ordering from the A2 to the  $L2_1$  structure is suppressed by quenching and the martensitic transformation from the A2 to the 2M occurs at low temperature [8].

Very recently, the present authors have demonstrated that SM and SE effects can be enhanced by microstructural control such as grain size and texture control and that a SE strain of about 8% can be obtained in Cu-Al-Mn-based SMAs [11-14]. Moreover, it has been found in these alloys that the hardness and strength significantly increase by ageing at around 300°C due to bainitic transformation [15]. Based on these findings, we have attempted to control the mechanical properties of the tip and the end portions

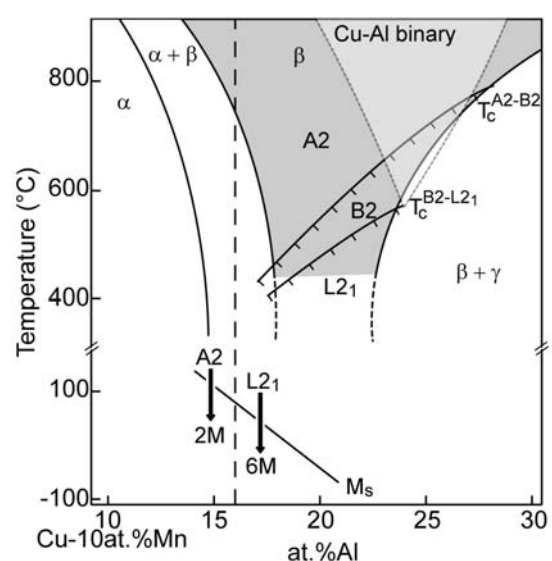


Fig. 1. Vertical section of the Cu-Al-Mn system at 10at.%Mn.

of Cu-Al-Mn-based wire individually by microstructural control. In this article, a new class of medical guidewire possessing functionally graded characteristics is presented.

## 2. Experimental procedure

Cu-Al-Mn-based alloys with a composition of  $\text{Cu}_{71}\text{Al}_{18}\text{Mn}_{11}$ ,  $\text{Cu}_{70.4}\text{Al}_{17.5}\text{Mn}_{12}\text{Si}_{0.1}$ ,  $(\text{Cu}_{72}\text{Al}_{17}\text{Mn}_{11})_{99.8}\text{B}_{0.2}$ ,  $(\text{Cu}_{72.5}\text{Al}_{17}\text{Mn}_{10.5})_{99.5}\text{Co}_{0.5}$  and  $(\text{Cu}_{72.0}\text{Al}_{17.5}\text{Mn}_{10.5})_{99.5}\text{Co}_{0.5}$  (at.%) were prepared by induction melting in an argon atmosphere. Si and B were added to raise the martensitic transformation temperatures and to obtain specimens with fine grains, respectively [16,17]. A large grain size was obtained for a specimen containing Co by secondary recrystallization [16]. The ingots were hot-rolled at 800°C and then cold-rolled. Wires were then obtained by cold-drawing with annealing at 600°C. The obtained Cu-Al-Mn-based wires were solution-treated at around 800°C - 900°C and then aged in a temperature range of 200°C to 450°C in air. The microstructures were observed by optical microscopy (OM). The crystal structure and the composition of precipitates were examined by X-ray diffraction (XRD) and scanning transmission electron microscopy with an energy dispersive spectroscopy (STEM-EDS), respectively. The SE property was examined by tensile testing using an Instron machine at a strain rate of  $0.83 \times 10^{-2}$  mm/s at room temperature. The gauge-length of the tensile specimen was 50 mm and the SE strains were measured using an extensometer. The hardness of specimens was determined by Vickers hardness (VH) measurement and the 3-point bending test was carried out at a strain rate of  $0.33 \times 10^{-1}$  mm/s at room temperature. A Cu-Al-Mn medical guidewire with functionally graded characteristics was manufactured based on the obtained results. A conventional experiment for estimating torquability of the Cu-Al-Mn-based guidewire was performed, where the details being given in the text.

## 3. Results and discussion

### 3-1. Superelasticity of Cu-Al-Mn SMA wires

We have shown that the SE strain of the sheet specimen is strongly dependent on the relative grain size  $d/t$ , where  $t$  and  $d$  are specimen thickness and mean grain diameter, respectively. Moreover, in the sheet specimen with columnar grains, large SE strain can be obtained because the volume ratio of the grains with a free

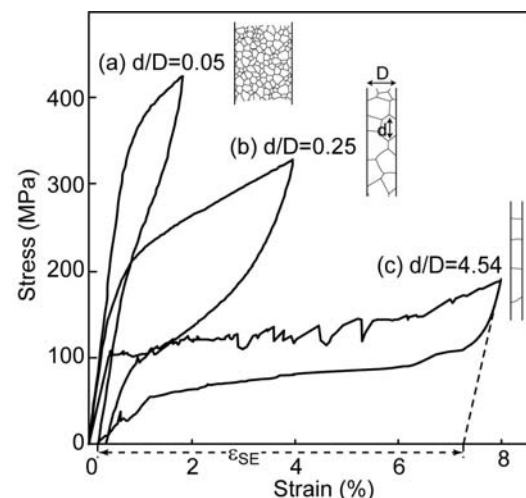


Fig.2. Tensile stress-strain curves at room temperature.

surface increases and the constraint strain from the surrounding neighboring grains drastically decreases [12]. This effect was also confirmed in the wire specimens with large grain size [14]. Figure 1 shows the stress-strain curve of the wire specimens with relative grain sizes of  $d/D = 0.05$ ,  $0.06$  and  $4.54$  for  $(\text{Cu}_{72}\text{Al}_{17}\text{Mn}_{11})_{99.8}\text{-B}_{0.2}$ ,  $(\text{Cu}_{72}\text{Al}_{17.5}\text{Mn}_{10.5})_{99.5}\text{-Co}_{0.5}$  and  $(\text{Cu}_{72.5}\text{Al}_{17}\text{Mn}_{10.5})_{99.5}\text{-Co}_{0.5}$ , respectively, where  $D$  is the diameter of the wire. It can be seen that the SE strain strongly depends on the relative grain size  $d/D$  and increases with increasing  $d/D$ , while the wire specimens with small  $d/D$  have large yield and tensile stresses as shown in Fig 2. These results suggest that the constraint stresses in the wire specimens with small  $d/D$  are larger than those with large  $d/D$  as well as those in the case of sheet specimens. The highest SE strain of about 7 % is obtained in the wire with a bamboo structure of  $d/D \gg 1$ , although the wire is not uniformly deformed as demonstrated in Fig. 2. Therefore, the relative grain size  $d/D$  should be kept slightly below  $d/D = 1$  in order to achieve high SE strain and to obtain uniform deformation. The present authors have recently reported that the grain size dependence of the yield stress and SE strain in Cu-Al-Mn-based SE wires can be predicted using a new model combined with the Taylor and the Sachs models, in which grain constraint effect is considered and ignored, respectively [14].

### 3-2. Effect of ageing on microstructure, hardness and bending properties

Figure 3(a) shows the effect of ageing temperature on VH of  $\text{Cu}_{71}\text{Al}_{18}\text{Mn}_{11}$  specimens, where the specimens were solution-treated at  $900^\circ\text{C}$  for 15 min followed by ageing at several temperatures for 15 min. The hardness drastically increases with increasing of aging temperature in the low temperature region and then decreases after reaching the maximum VH obtained by ageing at  $300^\circ\text{C}$ . Figures 3(b) - (d) show OM microstructures observed from the specimens aged at (b)  $200^\circ\text{C}$ , (c)  $300^\circ\text{C}$  and (d)  $350^\circ\text{C}$ . The specimen aged at  $200^\circ\text{C}$  is  $\beta$  single-phase, while the specimens aged at over  $300^\circ\text{C}$  show fine microstructures with plate-like precipitates in

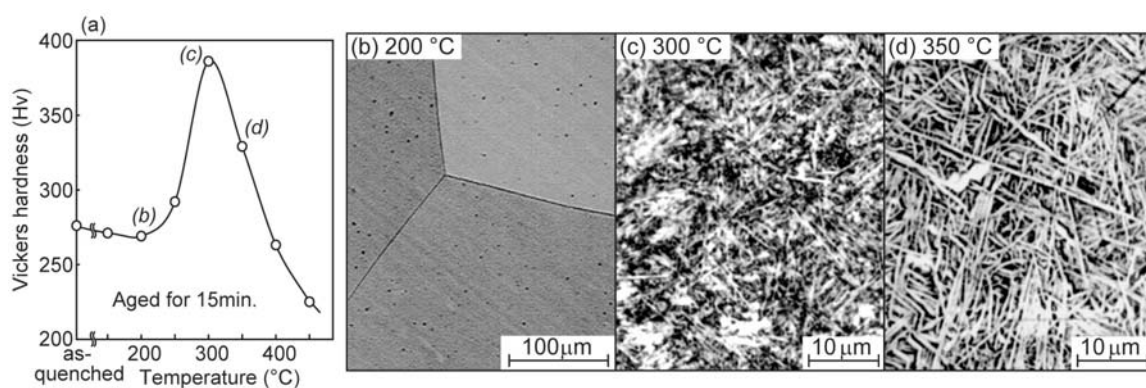


Fig. 3. (a) Plots of Vickers hardness vs. ageing temperature and microstructures of specimens aged at (b)  $200^\circ\text{C}$ , (c)  $300^\circ\text{C}$ , (d)  $350^\circ\text{C}$ , where (b)-(d) correspond to those in Fig. (a).

the  $\beta$  matrix and an increase in the size of precipitates with increasing the ageing temperature. It is confirmed by X-ray analysis and STEM-EDS observation that the plate-like precipitates have the long period stacking order structure, namely, the 9R structure, which is observed in the martensite phase transformed from the Cu-Al-Mn  $\beta_2$  (B2) phase. Moreover, the composition of precipitates is different from that of the  $\beta$  parent phase, which means that diffusion occurs during the formation of the precipitates. From these facts, it is supposed that the plate-like precipitates are due to bainitic transformation which has also been observed in other Cu-based alloys [18,19]. Furthermore, it was observed by X-ray analysis that the degree of order in the  $\beta_1$  (L2<sub>1</sub>) phase was increased by low temperature ageing. Consequently, it is concluded that the increment of the hardness by low temperature ageing is caused by the formation of a fine microstructure with bainite plates and the increase of the degree of order in the L2<sub>1</sub> phase, and that the decrement of the hardness is due to an increment in the size of the bainite plates.

Moreover, it is noted that the ductility of bainitic transformed  $\beta$  alloys can be improved by introduction of the  $\alpha$  (fcc) phase [20] as shown in Fig. 4. Such microstructure can be obtained by annealing in the  $\beta+\alpha$  two-phase region followed by the final low temperature ageing.

### 3-3.A new type of guidewire with functionally graded properties

A guidewire is indispensable for introducing a catheter into a blood vessel and is used for angiography, etc. The tip portion of the guidewire must have sufficient flexibility to pass through the meandering blood vessels, so that the catheter can be introduced into a desired site. On the other hand, in the body portion of the guidewire, high rigidity is required to overcome the high resistance to bending in a blood vessel and to smoothly transmit the torque from the end to the tip portion of the guidewire. At present, stainless steel and superelastic Ti-Ni wires are widely used for the core wire of the guidewire. Although the strength of stainless steel wire is very high, as shown in Fig. 5(a), its response to rotation is poor because plastic deformation easily occurs. On the other hand, Ti-Ni wire shows excellent flexibility due to the SE effect, as shown in Fig. 5(b), but its pushability and torquability are insufficient because of low stiffness. Therefore, a new class of guidewires with

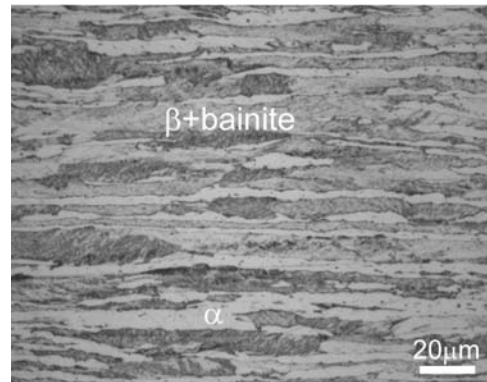


Fig.4. OM microstructure of age-hardened specimen with ductile  $\alpha$  phase.

advantages of both stainless steel and Ti-Ni wires is strongly required.

In the Cu-Al-Mn SMA, the mechanical properties can be varied by microstructural control as previously described. As can be seen from Fig. 5(c), the Cu-Al-Mn SE wire shows excellent superelasticity and is much softer than the Ti-Ni SE wire. On the other hand, the Cu-Al-Mn rigid wire aged at low temperature exhibits much higher strength than the Ti-Ni SE wire, as shown in Fig. 5(d), and its Young's modulus  $E$  is comparable to that of stainless steel wire.

In the present study, a functionally graded core wire with mechanical properties varying from the tip to the end

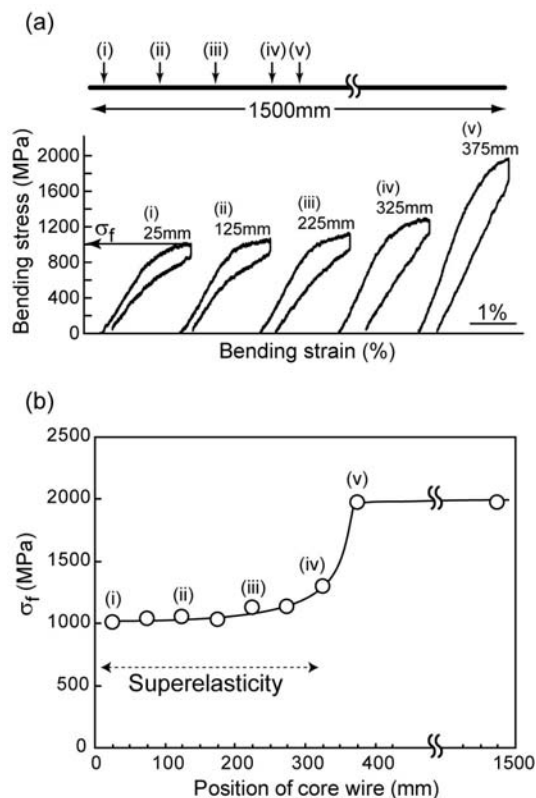


Fig.6. (a) Load-deflection curves obtained by a bending test at room temperature in the core wires with functionally graded properties. (b) Plots of  $\sigma_f$  vs. position of core wire, where  $\sigma_f$  is defined as shown in (a).

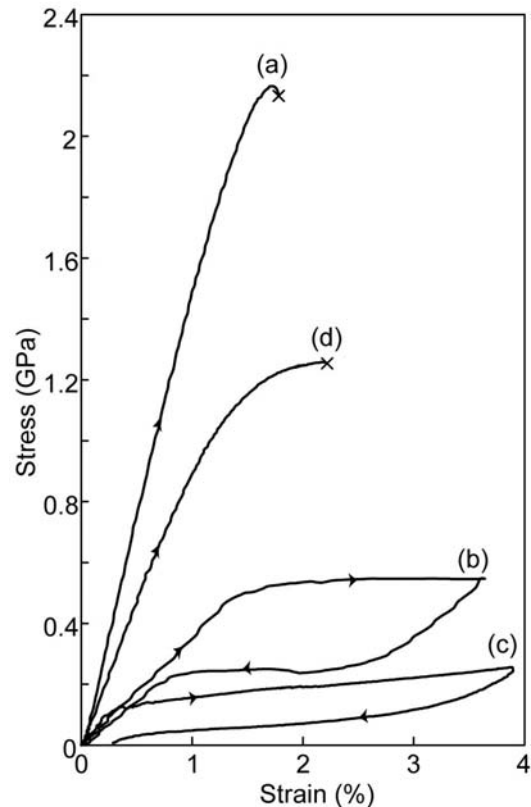


Fig.5. Stress-strain curves obtained by tensile-testing in (a) Stainless steel, (b) Ti-Ni, (c) Cu-Al-Mn-based SE and (d) Cu-Al-Mn rigid wires.

was prepared. Graded characteristics can be obtained by ageing in a temperature-graded furnace or by heat-treating the tip portion and the body portion of the core wire individually [16]. Figure 6(a) shows the load-deflection curves obtained from each part of  $\text{Cu}_{70.4}\text{Al}_{17.5}\text{Mn}_{12}\text{Si}_{0.1}$  wire with functionally graded characteristics, where only the tip portion of the age-hardened wire with a length of 1500 mm was solution-treated at  $800^\circ\text{C}$  to obtain the SE. Furthermore, bending stress  $\sigma_f$  vs. position of core wire is shown in Fig. 6(b), where  $\sigma_f$  is the stress level when a bending strain of 2% is applied, as shown in Fig. 6(a). It can be seen that the tip portion of core wire is

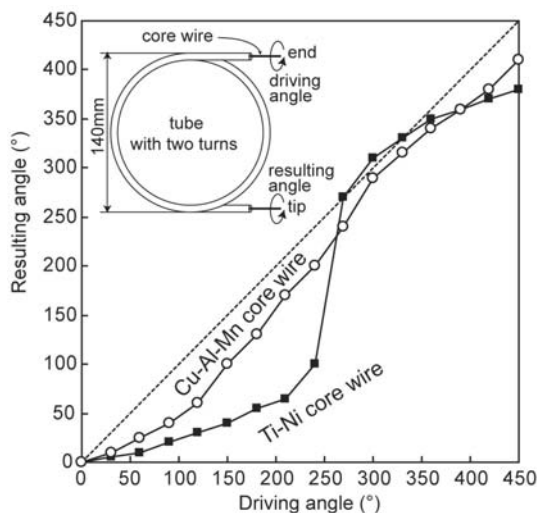


Fig.7. Plot of the resulting angle as a function of the driving angle in the Cu-Al-Mn-based and Ti-Ni core wires, where the inset shows an experimental method for measuring torquability.

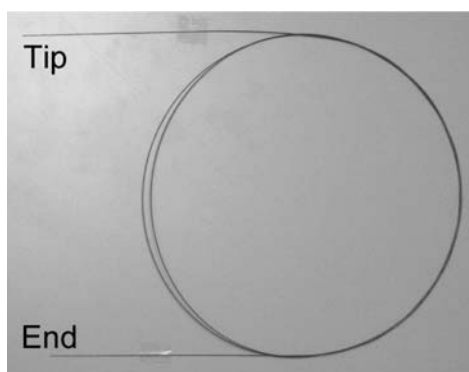


Fig.8. Cu-Al-Mn-based guidewire with functionally graded characteristics, where the guidewire is coated with resin.

considerably flexible showing SE and that the strength of the wire increases gradually in the range of 200 mm to 400 mm. Moreover, the body portion of the core wire possesses a high constant strength.

The torquability of this core wire was evaluated using a conventional method. The inset in Fig. 7 shows the experimental method used to investigate the torquability of the guidewire [21]. A circular Teflon tube with a diameter of 140 mm and two turns which simulates an imaginary blood vessel is prepared, the outside and inside diameters of the tube being 4 mm and 3 mm, respectively. The torquability is investigated by inserting a core wire with a length of 1500 mm into the Teflon tube. Details of this experimental method have been described in previous paper [16]. Figure 7 shows the experimental results on the torquability of the Cu-Al-Mn- based and Ti-Ni core wires, where the dotted line shows ideal torquability, i.e., the driving angle in the end portion of the guidewire completely agrees with the resulting angle in the tip of the guidewire. It is seen that the torquability of the Ti-Ni core wire is insufficient, because the plots of the resulting angle vs. the driving angle

considerably deviate from the ideal line and suddenly approach the ideal line when the driving angle becomes large. Such a phenomenon is called “Whipping” which is the most annoying guidewire problem, because if this phenomenon occurs, the blood vessel is significantly damaged by the sudden, large rotation of the guidewire. On the other hand, the present Cu-Al-Mn-based core wire with functionally graded characteristics shows excellent torquability, and the results are almost coincident with the ideal line because the body portion of the core wire has a high rigidity. A photograph in Fig. 8 shows a real Cu-Al-Mn-based guidewire having functionally graded characteristics. Usually, a hydrophilic coating is applied to facilitate smooth

movement of the guidewire in the blood vessel. It was confirmed that liquation of the metal elements into blood vessel can be suppressed by such coating.

As shown by these results, the herein presented Cu-Al-Mn-based guidewire with functionally graded characteristics has considerably better handling ability than the stainless steel and the Ti-Ni guidewires and show promise as a new type of guidewire. This Cu-Al-Mn-based guidewire is now under evaluation by doctors.

#### **4. Conclusions**

The manufacturing of a Cu-Al-Mn-based guidewire with mechanical properties such as SE, stiffness and strength graded from the tip to the end was attempted. The results obtained are as follows.

1. SE of the Cu-Al-Mn-based SMAs is improved by the control of relative grain size and such SE wires are softer than Ti-Ni SE wires. Moreover, the Cu-Al-Mn-based alloys show a significant increase of hardness by ageing at around 300°C and the strength and stiffness of those wires are comparable to those of stainless steel wire.
2. The torquability of such Cu-Al-Mn-based guidewires with functionally graded characteristics is superior to those of the stainless steel and the Ti-Ni guidewires.

#### **Acknowledgements**

This work was supported by the Industrial Technology Research Grant Program from NEDO, Japan. Partial support from the Encouraging Development Strategic Research Centers Program, the Special Coordination Funds for Promoting Science and Technology are also acknowledged. One of the authors (Y. S.) also acknowledges "IKETANI SCIENCE AND TECHNOLOGY FOUNDATION" for financial support.

#### **References**

1. K. Otsuka and X. Ren, *Intermetallics*, 7 (1999) 511-528.
2. S. Miyazaki, in *Shape Memory Materials*. Otsuka K, Wayman C. M, eds. Cambridge: Cambridge University Press; 1998, p. 267.
3. T. Duerig, A. Pelton and D. Stöckel, *Mater. Sci. Eng. A*, 273-275 (1999) 149-160.
4. J. Stice, in *Engineering Aspects of Shape Memory Alloys*. T. Duerig, K. Melton, D. Stöckel, C. Wayman, eds. London: Butterworth-Heinemann Ltd.; 1990. p. 483-487.
5. T. Tadaki, in *Shape Memory Materials*, K. Otsuka and C. M. Wayman, eds., Cambridge University Press, Cambridge, 1998, p. 97-116.
6. J. Van Humbeeck and L. Delaey, in *The Martensitic Transformation in Science*



- and Technology, E. Hornbogen and N. Jost, eds., Butterworth-Heinemann, England, 1990, p. 15-25.
7. S. Miyazaki and K. Otsuka, *ISIJ Int.*, 29 (1989) 353-376.
  8. R. Kainuma, S. Takahashi and K. Ishida, *Metall. Mater. Trans. A*, 27A (1996) 2187-2195.
  9. R. Kainuma, S. Takahashi and K. Ishida, *J. Phys. IV*, 5(C8) (1995) 961-966.
  10. R. Kainuma, N. Satoh, X. J. Liu, I. Ohnuma and K. Ishida, *J. Alloys Comp.*, 266 (1998) 191-200.
  11. Y. Sutou, T. Omori, R. Kainuma, N. Ono and Ishida K, *Metall. Mater. Trans. A*, 33 (2002) 2817-2824.
  12. Y. Sutou, T. Omori, J. J. Wang, R. Kainuma and K. Ishida, *J. de Phys. IV*, 112 (2003) 511-514.
  13. Y. Sutou, T. Omori, J. J. Wang, R. Kainuma and K. Ishida, *Mater. Sci. Eng. A*, 378 (2004) 278-282.
  14. Y. Sutou, T. Omori, K. Yamauchi, N. Ono, R. Kainuma and K. Ishida, *Acta Mater.*, 53 (2005) 4121-4133.
  15. Y. Sutou, Ph. D. Thesis, Tohoku University, Sendai, Japan, 2001.
  16. Y. Sutou, T. Omori, A. Furukawa, Y. Takahashi, R. Kainuma, K. Yamauchi, S. Yamashita and K. Ishida, *J. Biomed. Mater. Res., Part B: Applied Biomaterials*, 69B (2004) 64-69.
  17. Y. Sutou, R. Kainuma, K. Ishida, *Mater. Sci. Eng. A*, 273-275 (1999) 375-379.
  18. K. Takezawa, S. Sato, *Metall. Trans. A*, 21 (1990) 1541-1545.
  19. K. Takezawa, S. Sato, *Mater. Trans. JIM*, 33 (1992) 102-109.
  20. Y. Sutou, T. Omori, A. Furukawa, M. Suzuki, K. Yamauchi, R. Kainuma, and K. Ishida, unpublished work.
  21. Ueki T. *Boundary*, 3 (1996) 28-31. (in Japanese)